Experimental study of clear-water contraction scour

Ravindra Kumar Singh, Manish Pandey, Jaan H. Pu, Srinivas Pasupuleti and Vasanta G. Kumar Villuri

ABSTRACT

In this paper, experimental results of clear-water scour on a sand bed under short contractions were studied. Sequences of test runs were performed under clear-water conditions for three different contraction ratios. The outcomes of the experiments were employed to define the effects of various parameters on equilibrium scour depth under clear-water scour conditions. In this work, the precision of three maximum scour depth equations was tested from previous studies for contraction scour cases. Two new analytical equations were proposed to calculate time-dependent scour depth and maximum scour at equilibrium conditions, respectively, from the study. The proposed equations were validated using measurements from the present study as well as from previous literature, and the equations show a reasonable agreement between measured and computed values of scour depth under clear-water conditions in short contraction. The presented equations can be used for studying protection of the submerged portion at a bridge abutment or any similar structure.

Key words | clear-water scour, contraction scour, maximum scour depth, time-dependent scour depth

Ravindra Kumar Singh
Srinivas Pasupuleti
Department of Civil Engineering,
IIT (ISM),
Dhanbad,
India

Manish Pandey (corresponding author)
Department of Civil Engineering,
National Institute of Technology (NIT) Warangal,
India
E-mail: *manishpandey3aug@gmail.com*

Jaan H. Pu
Faculty of Engineering and Informatics,
University of Bradford,
Bradford BD7 1DP,
UK

Vasanta G. Kumar Villuri
Department of Mining Engineering,
IIT (ISM),
Dhanbad,
India

INTRODUCTION

Throughout the centuries, the failure of bridges always has significant societal and economic consequences. Lack of knowledge regarding bridge construction in natural streams or rivers leads to reduced working-life and increased damage to the bridge and its various parts.

Bed scouring in a stream near a bridge abutment is the key root cause of its failure (Barbhuiya & Dey 2004; Azamathulla *et al.* 2009). In the categories of scour, general scour refers to the haphazard removal of sediment from the channel bed by the high discharge of water irrespective of the location of riverine structure; whereas local scour is the localized removal of streambed material by erosive action of flowing water around obstructive structures, i.e. pier and abutment. By definition, contraction scour falls in the category of local scour, which occurs due to bridge pier and abutment that cause flow acceleration surrounding them. Due to flow acceleration near the contracted zone, bed shear stress also increases in this zone. As soon as this bed shear stress surpasses the critical shear stress, the scour process will start. As proposed by Azamathulla *et al.* (2008) and Kothyari *et al.* (2007), a 3-D separation of the boundary layer occurs near bridge components like pier and abutment. This further points out that vortex generation due to the movement of a separated shear layer in an upward direction near the upstream obstructed segment and the connected downflow by the stream can cause scour at the pier and abutments.

Contraction may be short or long, depending on the ratio of the longitudinal length of the abutment (L) to the channel width (B). Different researchers have selected varying ratios for defining contraction as short or long contraction, e.g. Raikar (2004) has suggested that a long contraction should have a ratio greater than or equal to 1.

doi: 10.2166/ws.2020.014

The present study deals with the contraction scour for clear-water conditions, in which three different contraction ratios were used. Contraction ratio is the total transverse length of abutment (b) to the channel width (B), where the total transverse length of abutment is the sum of transverse lengths of each side abutment (l). For these tests, the time-dependent scour depth highlighted the impact of different contraction ratios in short contraction on maximum scour depth. As outlined by Pu & Lim (2014) and Pu *et al.* (2014), the study of scouring up to the equilibrium stage is crucial to revealing the true scouring characteristics. In this study, novel equations to represent time-dependent scour depth were proposed. All the experiments were run until the equilibrium stage.

EXPERIMENTAL SETUP AND PROCEDURE

The laboratory experiments were run in a 24.0 m long, 1.0 m wide and 0.50 m depth fixed bed masonry flume. A working section of 4 m length (at 14.7 m downstream from the flume entrance) was prepared by filling with cohesionless sand for conducting the experiments. The emerged impervious rectangular abutments were used in the working section, which had transverse length on each side (l) of 0.10 m, 0.20 m and 0.30 m and longitudinal length of abutment (L) of 0.20 m. The abutments were immovably fixed at right angles to the flume wall for all experiments. The upstream face of the abutments was fixed at 15.7 m from the flume entrance. For all experiments in this study, the contraction ratios were employed as 0.2, 0.4 and 0.6. The inflow into the flume was controlled by an inlet valve and discharge was measured by a sharp crested weir located at the end of the flume. The required water depth in the flume was achieved by adjusting a tailgate located at the downstream end of the flume.

Water depth was measured with the help of a Vernier point gauge that had an accuracy of ±0.1 mm. The sand bed at the flume was levelled with respect to the channel slope, and a Perspex sheet was used to cover the bed around the abutment to prevent initial scour. A pre-determined discharge was used in the flume with the maintained water depth of 10 cm achieved by the end tailgate. Once the pre-set discharge and hydraulic parameters were attained, the Perspex sheet was carefully removed without disturbing the channel bed. Then, the measurement of temporal scour depth was started. A Vernier point gauge was used to measure scour depth at varying time intervals until the scouring achieved an equilibrium condition.

In the present study, a total of nine experimental runs were conducted using sand of 0.27 mm median diameter (d_{50}) and 1.25 geometric standard deviation (σ). Three different discharges (Q1, Q2 and Q3) were used in experiments for each contraction ratio test. All experiments were run under clear-water scour conditions, meaning $U/U_c < 1$. Here U is approach mean velocity and U_c is the critical velocity for the sediment defined by Lauchlan & Melville (2001) as follows:

$$\frac{U_c}{U_{*c}} = 5.75\left(\frac{y}{k_s}\right) + 6 \quad (1)$$

where y = approaching flow depth, $k_s = 2d_{50}$ (equivalent roughness height) and U_{*c} = critical shear velocity of sediment calculated by the Shields method (refer to Pu *et al.* 2017, 2018). All the hydraulic and geometric parameters employed in the present study are listed in Table 1.

RESULTS AND DISCUSSION

Time-dependent scour depth

Estimation of time-dependent scour depth (d_{st}) around the abutments in the tested contraction cases is discussed

Table 1 | Geometric and hydraulic parameters of the experimental setup

Length of flume	24 m
Flume width (B)	1 m
Longitudinal length of abutment (L)	0.20 m
Transverse length of each side abutment (l)	l = 0.10–0.30 m
Total transverse length of abutment (b)	$b = 2l$ = 0.20–0.60 m
Flow depth (y)	0.1 m
Discharge (Q)	16.51–21.51 l/s
Approach mean velocity (U)	0.165–0.215 m/s
Critical velocity ratio (U/U_c)	0.63–0.84
Median diameter of sand, d_{50}	0.27 mm
Standard deviation of particle distribution (σ)	1.25

here. In the present experimental study, an attempt was made to develop a clear-water time-dependent scour relationship for the temporal scour depth measured at the upstream nose of an abutment.

Theoretical background

Parameters that affect the time-dependent scour depth at an abutment due to contraction of flow can be listed as the geometry, transverse length of the abutment, sediment, approach flow properties and time of scour. Temporally varying scour depth (d_{st}) around an abutment for the contraction case can hence be written as:

$$d_{st} = f(d_{50}, \sigma, \rho_s, U_c, \rho, \nu, U, y, L, l, b, t, T) \quad (2)$$

In Equation (2), the flow parameters are (ρ, ν, U, y), abutment geometry and contraction parameters are (L, l, b), sediment parameters are (d_{50}, σ, ρ_s, U_c) and time parameters are (t, T), where d_{50} is median diameter of sediment and σ is respective geometric standard deviation, ρ_s is sediment density, U_c is critical mean velocity, ρ is fluid density, ν is kinematic viscosity of fluid, U is approach mean velocity, y is approach flow depth, l is transverse length of each side abutment, L is the longitudinal length of abutment and $b = 2l$ is total transverse length of abutment, i.e. contraction width, d_{st} is the maximum scour depth at time t and T is the non-dimensional time parameter given by $T = t\{(S-1)gd_{50}\}^{0.5}/R_L$. S is relative density, g is the gravitational acceleration and $R_L = (l^2 y)^{1/3}$ is reference length.

For sediment–fluid interaction, the parameters g, ρ_s and ρ should not appear as self-governing parameters; a better illustration is $(S-1)g$. Equation (1) can be written in non-dimensional form:

$$\frac{d_{st}}{b} = f\left(F_{d50}, \frac{y}{l}, \frac{b}{B}\right) \quad (2a)$$

where F_{d50} is densimetric Froude number and defined as $F_{d50} = U/\{(S-1)gd_{50}\}^{0.5}$, and b is total transverse length and defined as $b = 2l$.

A similar approach may be applied for maximum scour depth (d_s) by dropping the time parameter from the above equations.

The scour rate mainly depends on the difference between critical and total shear stress. Thus, it is only sensible to relate the scour to time, where the time is t and the non-dimensional time function $f(t)$ on the right side of Equation (2) increases with time. Figure 1(a)–1(c) illustrate the variations of scour depth with time for different cases of contraction ratios. It is observed that during the initial stage, scouring around the abutment is very rapid; after 20% of the equilibrium time it gradually reduces. This scouring-stage-change finding agrees with the majority of literature findings, e.g. Pu & Lim (2014). With the increase in approach velocity, the scour depth increases with time

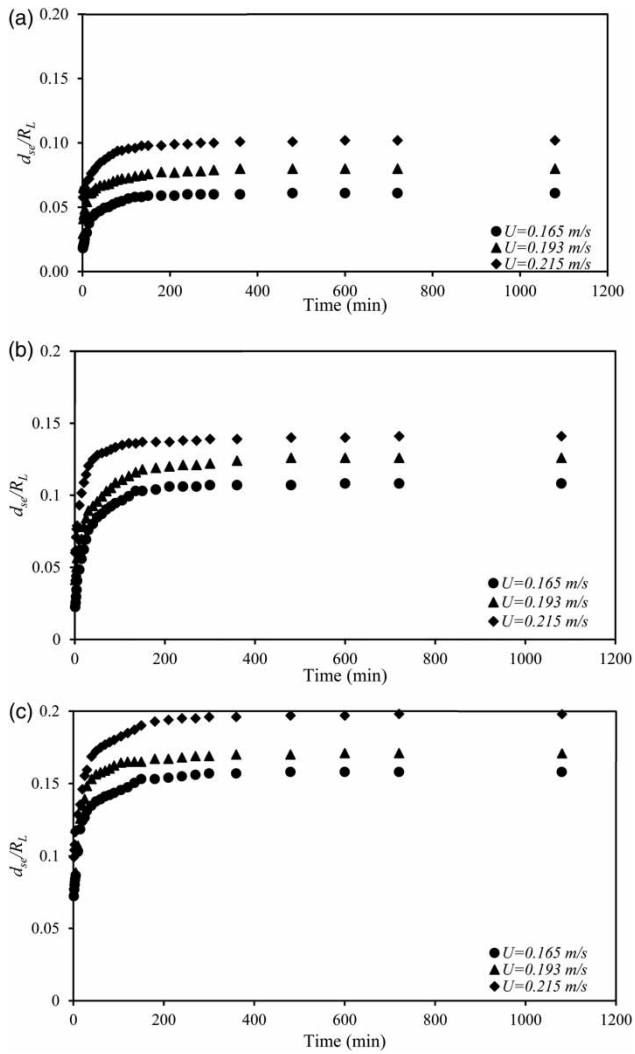

Figure 1 | Variation of scour depth with time; (a) $b/B = 0.2$, (b) $b/B = 0.4$, and (c) $b/B = 0.6$.

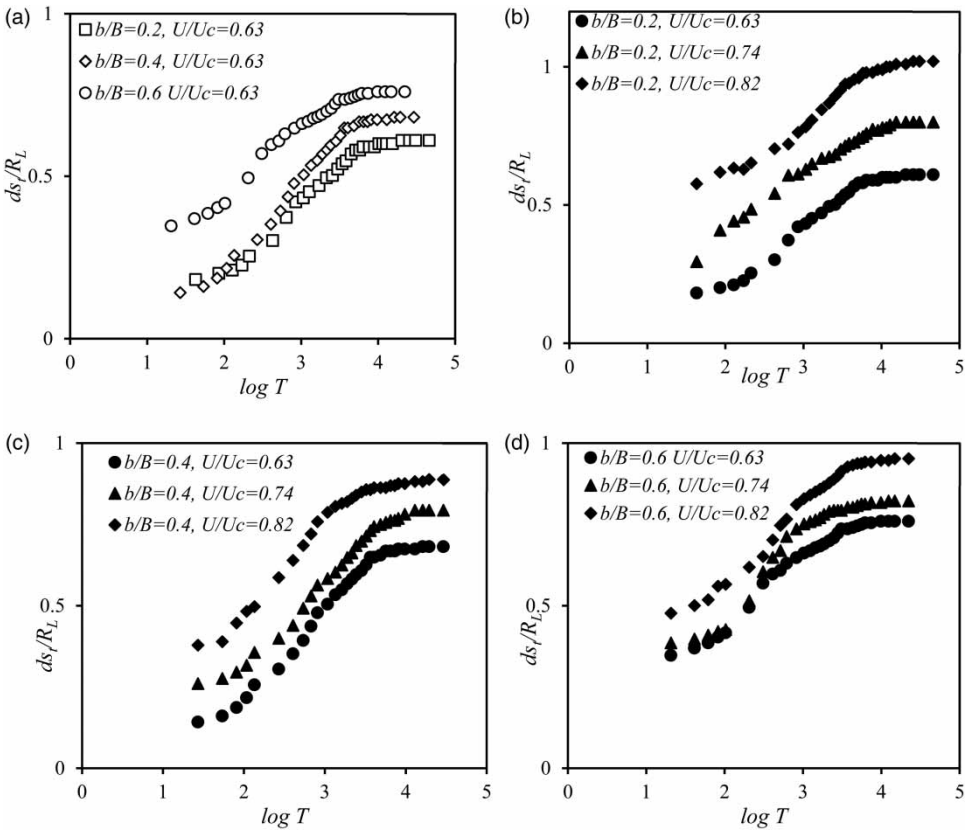

Figure 2 | Variation of scour depth with T; (a) $U/U_c = 0.63$, (b) $b/B = 0.2$, (c) $b/B = 0.4$, and (d) $b/B = 0.6$.

during the experimental duration. Figure 2 shows that the non-dimensional temporal-scour depth increases with time (t). It was also found that the time-dependent scour depth increases with the increase of contraction ratio (b/B) and critical velocity ratio (U/U_c), as illustrated in Figure 2(a)–2(d). Similar results were obtained by previous studies on various pier scour cases (Kothyari *et al.* 2007; Pandey *et al.* 2017, 2018a, 2018b).

The variation of time-dependent scour depth at the upstream nose of the abutment for contraction scour is illustrated in Figures 1 and 2 for different contraction ratio cases. The temporal measurements of scour depth

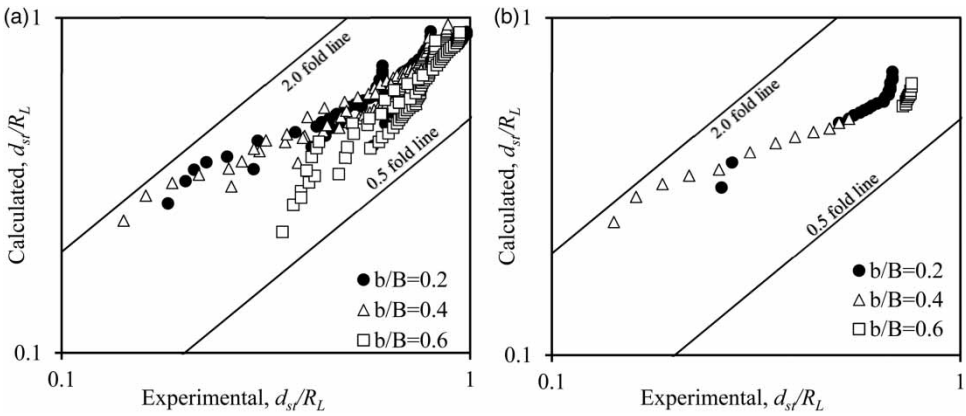

Figure 3 | Experimental vs calculated time-dependent scour depths using (a) calibration datasets and (b) validation datasets.

were performed at the upstream nose of the abutment, where maximum scour depth was observed. An attempt was made to develop a time-dependent scour depth equation using more than 300 temporal laboratory datasets measured in this study. Among the data, 70% of datasets were used for calibration and the remaining 30% of datasets for validation. Using the 70% calibration datasets, an empirical equation was derived (Equation (3)) to compute scour depth at different time intervals. Nonlinear regression analysis was also performed to obtain this equation.

$$\frac{d_{st}}{R_L} = 5.7(F_{d_{50}})^{1.5}(\log T)^{0.9}\left(\frac{y}{l}\right)^3\left(\frac{b}{B}\right)^3 \quad (3)$$

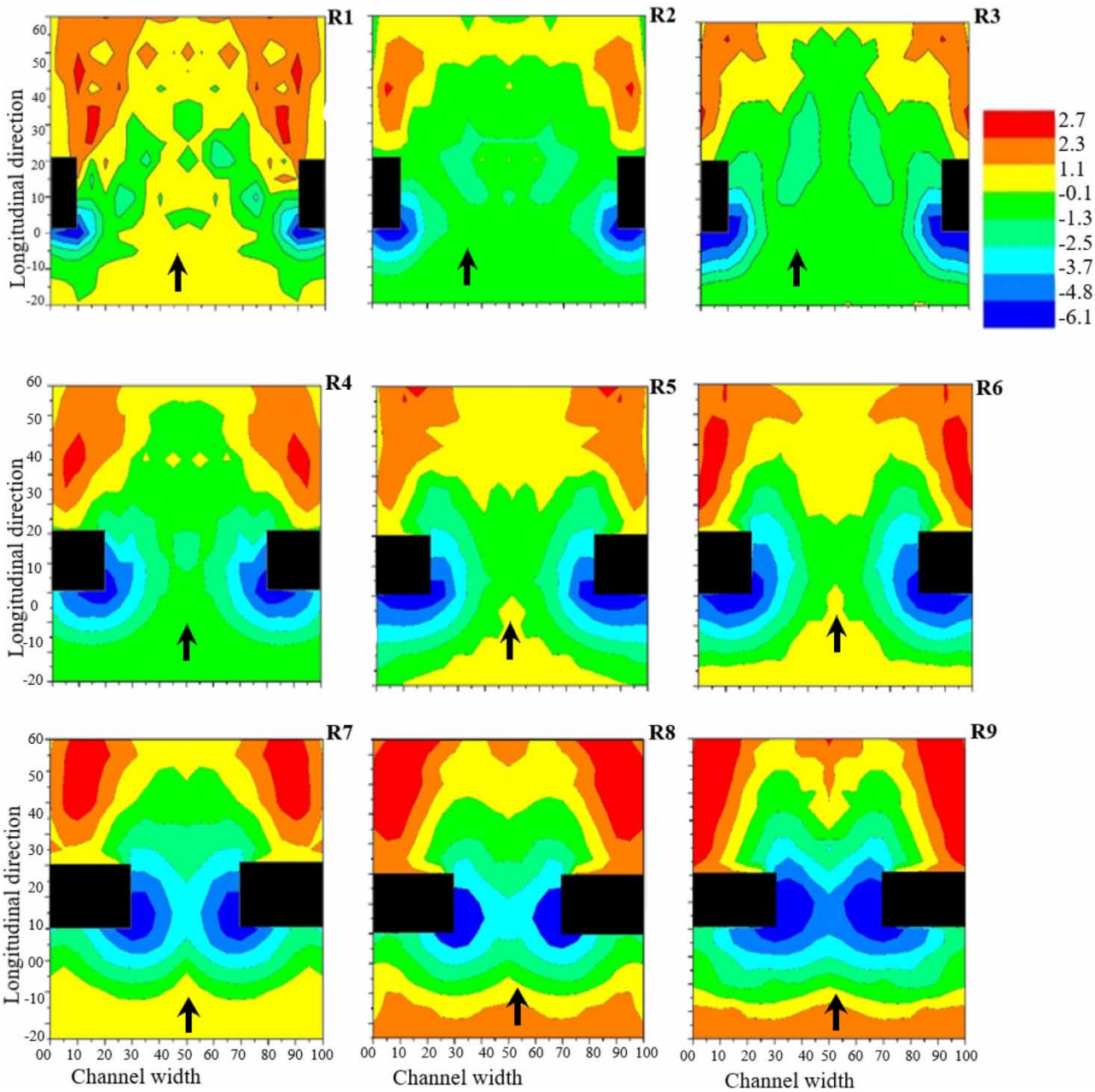

Figure 4 | Scour pattern at equilibrium scour condition (all dimensions are in cm) (refer to Table 3).

Here, reference length $R_L = (l^2 y)^{1/3}$, densimetric Froude number $F_{d50} = U/\{(S-1)gd_{50}\}^{0.5}$, $\Delta = S - 1$, S is relative density of sediment, i.e. 2.65, and $b = 2l$.

The value of the determination coefficient (R^2) of this equation is 0.91 for the validation datasets, which indicates its accuracy. Figure 3(a) and 3(b) illustrate the 0.5–2.0 fold lines between the observed and computed time-dependent non-dimensional scour depths using Equation (3). The time-dependent scour depths computed using Equation (3) show good agreement with observed data – both the calibrated as well as validated datasets, as illustrated in Figure 3(a) and 3(b).

Maximum scour depth at equilibrium condition

Detailed analysis of scour depth variation in the present study is presented in this section. It can be observed that the scour process happened swiftly during its initial stage, but after the passage of 25%–30% of the total time, the scour rate was very slow, as shown in Figure 1(a)–1(c). In the present study, maximum scour depth was measured with the help of a point gauge with ±0.1 mm accuracy. The location of maximum scour depth can be observed by the contour patterns of the flume bed drawn for all the experimental runs in Figure 4. Negative values in Figure 4 show the scour depth around the abutments, while positive values show the deposited sediment height. From the contour plot, it can be seen that the maximum equilibrium scour depth always occurred at the upstream abutment nose.

The authors observed that the maximum equilibrium scour depth increases with increase in contraction ratio. Figure 5 shows the effects of contraction ratios on maximum scour depth at the equilibrium stage, and for a fixed value of velocity, the maximum scour depth increases with contraction ratio. Also, for a constant value of contraction ratio, the maximum scour depth increases with increase in the approach mean velocity.

Previous maximum scour depth equations

Few previously suggested analytical equations were available for maximum scour depth computation in contraction scour conditions, i.e. Laursen (1963), Gill (1981) and Lim (1993), as shown in Table 2. These suggested relationships were analyzed to examine their performances. Nine present experimental datasets were used along with 63 datasets collected from previous studies for this test. The range of parameters in the present and previous datasets are summarized in Tables 3 and 4, respectively.

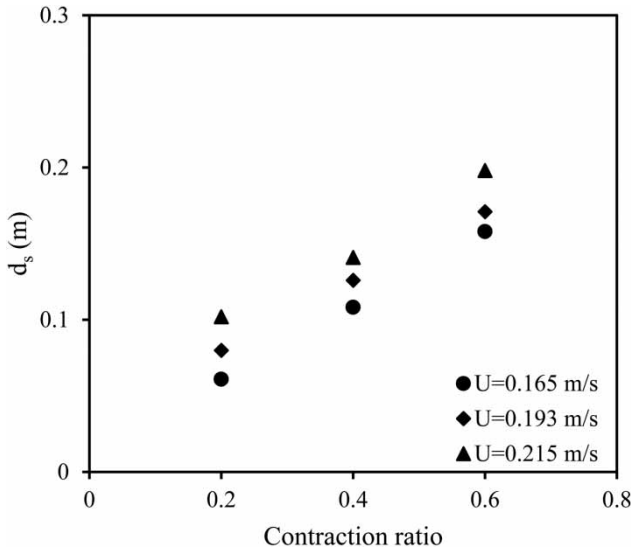

Figure 5 | Variation of scour depth with contraction ratio.

Figure 6(a)–6(c) compare experimental and calculated values of maximum equilibrium non-dimensional scour depth using previous equations. Figure 6(a) shows the experimental and calculated non-dimensional maximum scour depths using the equation by Laursen (1963). Only 20% of data were found to be within the 0.5–2.0 fold lines. Laursen (1963) did not include particle size and approach flow

Table 2 | Equations of maximum equilibrium scour depth proposed by different investigators

Researcher	Proposed relationship
Laursen (1963)	$\frac{d_s}{y} + 1 = \left(\frac{b}{B}\right)^{-0.875}$
Gill (1981)	$\frac{d_s}{y} + 1 = 1.58\left(\frac{b}{B}\right)^{-0.875}$
Lim (1993)	$\frac{d_s}{y} + 1 = 1.85(F_{d_{50}})^{0.75}\left(\frac{b}{B}\right)^{-0.75}\left(\frac{d_{50}}{By}\right)^{0.25}$
Present study	$\frac{d_s}{R_L} = 0.1(F_{d_{50}})^{0.6}\left(\frac{b}{B}\right)^{-1.1}$

Table 3 | Maximum scour depth and other hydraulic data pertaining to present study

Exp. run	d_{50} (mm)	U (m/s)	l (m)	b/B	F_{d50}	d_s (cm)
R1	0.27	0.165	0.1	0.2	2.49	6.13
R2	0.27	0.192	0.1	0.2	2.91	7.99
R3	0.27	0.215	0.1	0.2	3.25	10.03
R4	0.27	0.165	0.2	0.4	2.49	10.82
R5	0.27	0.192	0.2	0.4	2.91	12.56
R6	0.27	0.215	0.2	0.4	3.25	14.13
R7	0.27	0.165	0.3	0.6	2.49	15.77
R8	0.27	0.192	0.3	0.6	2.91	17.04
R9	0.27	0.215	0.3	0.6	3.25	19.81

velocity in his derivation, which consequently gave large comparison errors with the utilized experimental scour depths. Figure 6(b) illustrates the experimental versus calculated scour depths using the Gill (1981) analytical approach. Approximately 40% of datasets were found to be within the 0.5–2.0 fold lines, as the Gill (1981) proposed method also neglected particle size and approach velocity. Lim (1993) proposed an improved equation for contraction scour by including the particle size and approach flow velocity parameters. Figure 6(c) shows observed and computed scour depths using the Lim (1993) approach that have around 80% of datasets within the 0.5–2.0 fold lines. For calculating the maximum scour depth for contraction conditions, the equation proposed by Lim (1993) is more precise as compared with those of Laursen (1963) and Gill (1981). Lim (1993) stated that the contraction ratio and densimetric Froude number have a major influence on the scour process and hence have to be considered in the analytical equation. Figure 7 illustrates the variation of total number of percentage data and error for different equations. It can be noted that the relationship proposed by Lim (1993) performs better than other previous relationships. The Lim (1993) equation shows 50% data within ±25% error, whereas Gill (1981) and Laursen (1963) show only 30% and 20% data under ± 25%, respectively; while the present equation shows the least error and 70% data frequency lies under ±25% error.

A new non-dimensional maximum scour depth equation

In the previous studies, researchers stated that the scour processes under contraction conditions were significantly different from non-contraction conditions because of the influence of the contraction ratio (Dey & Raikar 2005; Ballio *et al.* 2009). Similar observations can also be made in the present study. By comparing the accuracy of previous maximum scour depth equations, a relatively large error between experimental and calculated values of scour depth can be found. Hence, this study further derives a new mathematical equation to compute the maximum scour depth under equilibrium conditions. For developing this new relationship, a sensitivity analysis was conducted, and the outcomes are presented in Table 5. A nonlinear regression analysis was performed after the sensitivity analysis, using 70% of present and previous maximum scour depth datasets for calibration and the remaining 30% of datasets for validation purposes of the equation. Equation (4) was derived to calculate the maximum scour depth under contraction conditions; the results from Equation (4) proved that the contraction ratio (b/B) and densimetric Froude number have a major impact on the maximum scour depth, as demonstrated in Figure 7 and Figure 8(a)

Table 4 | Maximum scour depth and other hydraulic data pertaining to previous studies

Investigators / Parameters	l (m)	y (m)	U (m/s)	b/B	d_{50} (mm)
Komura (1966)	0.05–0.1	0.032–0.084	0.17–0.25	0.25–0.5	0.35–0.55
Gill (1981)	0.25	0.038–0.084	0.28–0.39	0.65	0.92–1.53
Webby (1984)	0.26	0.09–0.12	0.23–0.37	0.33	2.15
Lim (1993)	0.06–0.13	0.024–0.028	0.21–0.22	0.30–0.65	0.47
Dey & Raikar (2005)	0.18	0.126–0.13	0.33–0.57	0.60	0.81–2.54

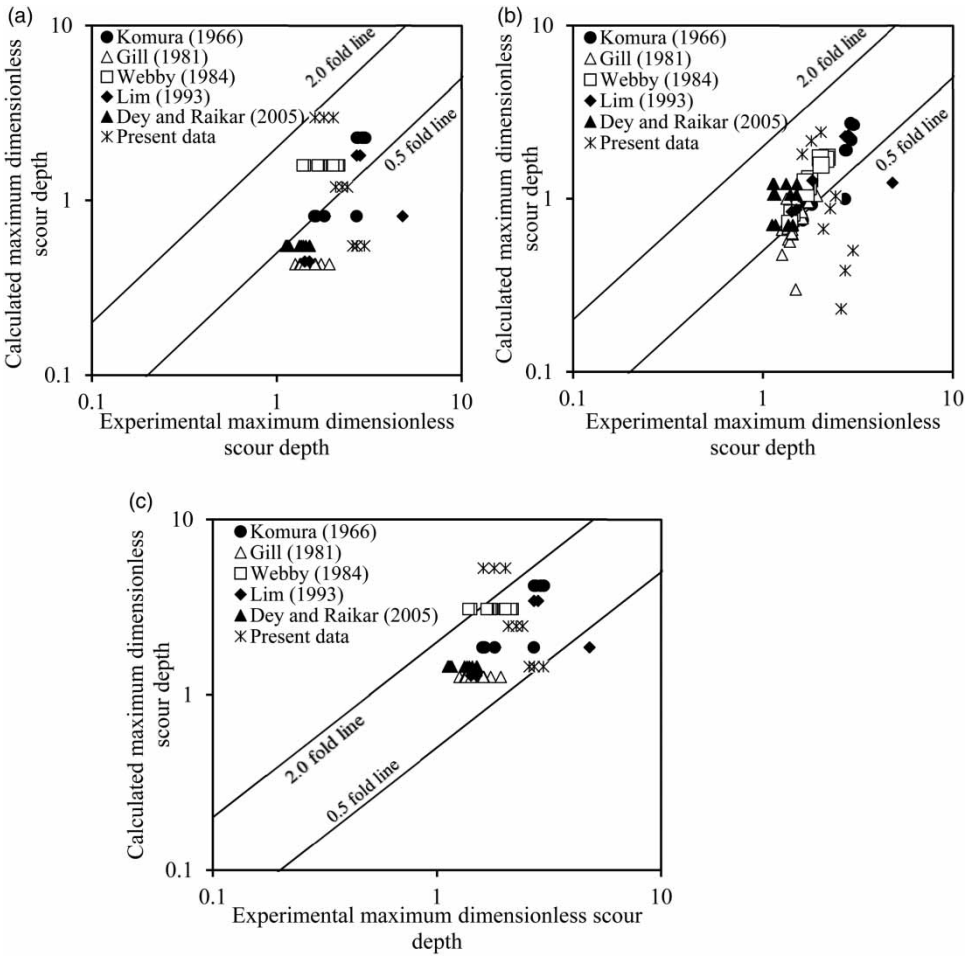

Figure 6 | Experimental versus calculated maximum dimensionless scour depths using the (a) Laursen (1963), (b) Gill (1981), and (c) Lim (1993) equations.

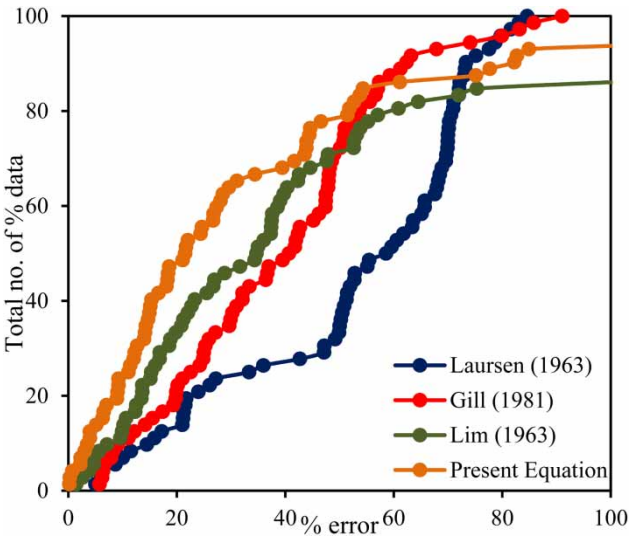

Figure 7 | Variation between percentage error and total percentage datasets.

Table 5 | Sensitivity analysis of present equation (where, *CD* is the coefficient of determination)

Functions	CD
$\frac{d_s}{R_L} = f\left\{(F_{d_{50}}), \left(\frac{b}{B}\right)\right\}$	0.91
$\frac{d_s}{R_L} = f\left\{(F_{d_{50}}), \left(\frac{b}{B}\right), \left(\frac{l}{d_{50}}\right)\right\}$	0.88
$\frac{d_s}{y} = f\left\{(F_{d_{50}}), \left(\frac{b}{B}\right)\right\}$	0.77
$\frac{d_s}{y} = f\left\{(F_{d_{50}}), \left(\frac{b}{B}\right), \left(\frac{l}{d_{50}}\right)\right\}$	0.76
$\frac{d_s}{b} = f\left\{(F_{d_{50}}), \left(\frac{b}{B}\right)\right\}$	0.73
$\frac{d_s}{b} = f\left\{(F_{d_{50}}), \left(\frac{b}{B}\right), \left(\frac{l}{d_{50}}\right)\right\}$	0.75

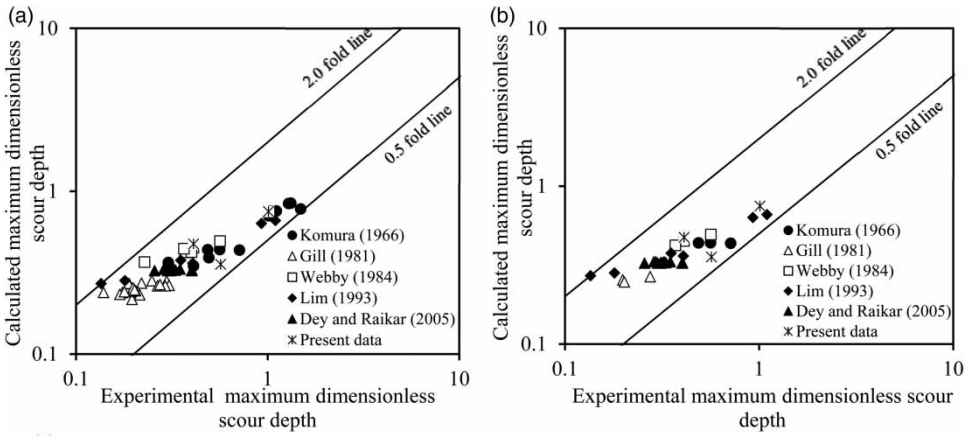

Figure 8 | Variation of experimental and calculated values of dimensionless scour depth using present relationship: (a) calibration datasets, and (b) validation datasets.

and 8(b). Certainly, the proposed equation has 100% of datasets within fold lines – better than previous equations.

$$\frac{d_s}{R_L} = 0.1(F_{d_{50}})^{0.6}\left(\frac{b}{B}\right)^{-1.1} \quad (4)$$

CONCLUSIONS

In the present experimental study, time-dependent as well as maximum equilibrium scour depths around abutments under short contraction scour were investigated. From this study, two equations for time-dependent scour and maximum equilibrium scour depth were derived. The comparison of experimental and calculated maximum equilibrium scour depths was conducted together with previously proposed equations. The important results and conclusions of this study are given below:

- A new relationship was derived to represent the time-dependent scour depth using the present experimental data. The derived equation was calibrated (using 70% of measured datasets) and validated (using 30% of measured datasets). This equation shows good agreement between experimental and calculated values of time-dependent scour depth.
- The rate of development of scour depth was rapid during the initiation of scour, which gradually decreased with time.
- The measured scour profile in the vicinity of the abutment indicated that the maximum scour depth occurs at its upstream nose. Also, it was found that the scour depth increased with the increase of contraction ratio.
- A maximum scour depth equation was proposed, calibrated and validated. It showed accurate results when comparing with previous equations.

REFERENCES

Azamathulla, H., Ghani, A., Zakaria, N. A., Lai, S. H., Chang, C. K., Leow, C. S. & Abuhasan, Z. 2008 Genetic programming to predict ski-jump bucket spill-way scour. *Journal of Hydrodynamics* **20** (4), 477–484.

Azamathulla, H., Ghani, A. A., Zakaria, N. A. & Guven, A. 2009 Genetic programming to predict bridge pier scour. *Journal of Hydraulic Engineering* **136** (3), 165–169.

Ballio, F., Teruzzi, A. & Radice, A. 2009 Constriction effects in clear-water scour at abutments. *Journal of Hydraulic Engineering* **135** (2), 140–145.

Barbhuiya, A. K. & Dey, S. 2004 Local scour at abutments: a review. *Sadhana* **29** (5), 449–476.

Dey, S. & Raikar, R. V. 2005 Scour in long contractions. *Journal of Hydraulic Engineering* **131** (12), 1036–1049.

Gill, M. A. 1981 Bed erosion in rectangular long contraction. *Journal of the Hydraulics Division* **107** (3), 273–284.

Komura, S. 1966 Equilibrium depth of scour in long constrictions. *Journal of the Hydraulics Division* **92** (5), 17–37.

Kothyari, U. C., Hager, W. H. & Oliveto, G. 2007 Generalized approach for clear-water scour at bridge foundation elements. *Journal of Hydraulic Engineering* **133** (11), 1229–1240.

Lauchlan, C. S. & Melville, B. W. 2001 Riprap protection at bridge piers. *Journal of Hydraulic Engineering* **127** (5), 412–418.

Laursen, E. M. 1963 An analysis of relief bridge scour. *Journal of the Hydraulics Division* **89** (3), 93–118.

Lim, S. Y. 1993 Clear water scour in long contractions. *Proceedings of the Institution of Civil Engineers – Water, Maritime and Energy* **101** (2), 93–98.

Pandey, M., Sharma, P. K., Ahmad, Z. & Singh, U. K. 2017 Evaluation of existing equations for temporal scour depth around circular bridge piers. *Environmental Fluid Mechanics* **17** (5), 981–995.

Pandey, M., Sharma, P. K., Ahmad, Z. & Karna, N. 2018a Maximum scour depth around bridge pier in gravel bed streams. *Natural Hazards* **91** (2), 819–836.

Pandey, M., Sharma, P. K., Ahmad, Z., Singh, U. K. & Karna, N. 2018b Three-dimensional velocity measurements around bridge piers in gravel bed. *Marine Georesources & Geotechnology* **36** (6), 663–676.

Pu, J. H. & Lim, S. Y. 2014 Efficient numerical computation and experimental study of temporally long equilibrium scour development around abutment. *Environmental Fluid Mechanics* **14**, 69–86.

Pu, J. H., Hussain, K., Shao, S. & Huang, Y. 2014 Shallow sediment transport flow computation using time-varying sediment adaptation length. *International Journal of Sediment Research* **29** (2), 171–183.

Pu, J. H., Wei, J. & Huang, Y. 2017 Velocity distribution and 3D turbulence characteristic analysis for flow over water-worked rough bed. *Water* **9** (9), 668.

Pu, J. H., Tait, S., Guo, Y., Huang, Y. & Hanmaiahgari, P. R. 2018 Dominant features in three-dimensional turbulence structure: comparison of non-uniform accelerating and decelerating flows. *Environmental Fluid Mechanics* **18** (2), 395–416.

Raikar, R. V. 2004 *Local and General Scour of Gravel Beds*. PhD thesis, Dept. of Civil Engineering, Indian Institute of Technology, Kharagpur, India.

Webby, M. G. 1984 General scour at contraction. *RRU Bulletin* **73**, 109–118.

First received 20 August 2019; accepted in revised form 21 January 2020. Available online 7 February 2020